Theoretical study of the thermochemistry of sulfur molecular crystals II. Lowest energy allotropes of polymeric ω-sulfurs†

Mohammed Ezzine,[a],‡ Alain Pellegatti,*[,a],§ Christian Minot,[b] Roland Jean-Marc Pellenq,[c] Josette Olivier-Fourcade[d] and Abdarrahim Boutalib[e]

[a] *Centre de Thermodynamique et de Microcalorimétrie (CNRS UPR 7461), 26 rue du 141ème R.I.A., 13331 Marseille cedex 3, France*
[b] *Laboratoire de Chimie Théorique (CNRS UMR 7616), Université Pierre et Marie Curie, 4 Place Jussieu, 75252 Paris cedex 05, France*
[c] *Centre de Recherche sur la Matière Divisée (CNRS UMR 6619), 1B rue de la Férollerie, 45071 Orléans cedex 02, France*
[d] *Laboratoire de Physicochimie de la Matière Condensée (CNRS UMR 5617), Université de Montpellier II, Place E. Bataillon, 34095 Montpellier cedex 5, France*
[e] *Département de Chimie, Université Cadi Ayyad, Faculté des Sciences, B.P. S15, Marrakech, Morocco*

Extended Hückel theory (for the repulsive part of the energy) and a method derived from classical perturbation expansions (for the long-range attractive part of the energy) were combined and the adequate parametrization has been set up in Part I. In this first part of the series, the method has been tested with success on ω-sulfur and on an example of two interacting helices. Here, we apply this method to determine the lowest energy conformations for all 1D, 2D and real 3D structures of polymeric ω-sulfurs considered from our structural hypotheses. We examine how considerations on the intermolecular repulsive interactions can lead to reliable structural information. Of course, the dispersive (attractive) part of the energy (including dipole-dipole, dipole-quadrupole and three-body terms) is necessary to determine quantitatively the stability of these sulfur structures. We find that ω_2-sulfur is more stable than ω_1-sulfur, where each of these helical chains is built up from a three-atom unit cell. For both 3D allotropes, the calculated enthalpy of sublimation is in good agreement with the experimental values.

Polymerized sulfur is one of the various allotropic forms of this element. It is used in the vulcanization process since, at variance with the most stable α form, it does not supersaturate upon cooling, which is responsible for the loss of adhesion of wires. Therefore, extensive knowledge about the structures of polymerized sulfur is interesting from both a fundamental and a practical point of view. We know that it is made of parallel and/or perpendicular infinite helical chains. However very recently, Cataldo,[1] on the basis of previous work,[2] stressed that the details of the structure are not entirely understood.

The polymerized forms of solid sulfur are characterized by their complete insolubility in carbon disulfide. Das,[3] Erametsa[4] and Tuinstra[5] were the pioneers in this research field. Tuinstra confirmed the presence of two different allotropes and called them $S_{\omega 1}$ and $S_{\omega 2}$. Following Pauling's proposals,[6] Tuinstra showed that only structures including helical chains as basic entities were satisfactory. Interpreting X-ray diffraction spectra on powder samples, he suggested that $S_{\omega 1}$ is in a pseudo-orthorhombic lattice shown in Fig. 1. Four helices, denoted **A**–**D**, are sufficient to reproduce all of the ω1 structure. He proposed that **A** and **C** are conrotatory helices (rotating both in the same direction; let us choose the right-hand one, for example: *rr*) and that **B** and **D** are also conrotatory with respect to each other but are rotating in the opposite direction (the left-hand one: *ll*). The structure of $S_{\omega 2}$ is based on a centred quadratic unit cell with successive parallel planes of helical chains where the axes of helices in one plane are perpendicular to those of helices in the two neighbouring ones. This *plywood* pattern explains some small interatomic distances between non-bonded atoms. The conformation, shown in Fig. 2, corresponds to a ten-atom elementary cell. The helices in a given plane, from the bottom to the top of the cell, are successively *r*-conrotatory and *l*-conrotatory. Twelve helices (three in each plane) are sufficient to describe the whole structure if one considers a ten-atom helical unit cell. In the case of a helical cell containing three atoms only, four helices (one in each plane) are sufficient to describe the structure.

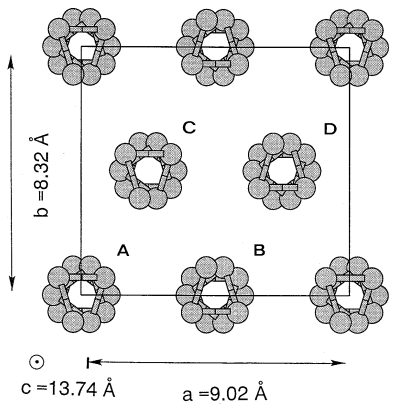

Fig. 1 Lattice structure of $S_{\omega 1}$ as proposed by Tuinstra.[5,10] We represent the helix with 10 atoms per cell along the direction *c*

† Part I is ref. 16 of this work.
Non-SI units employed: 1 eV ≈ 9.65 × 10^4 J mol^{-1}; 1 a.u. ≈ 2.63 × 10^6 J mol^{-1}.
‡ Also: Département de Chimie, Université Cadi Ayyad.
§ Present address: ENSSPICAM (CNRS UMR 6516), Faculté des Sciences de St Jérôme, Avenue Escadrille Normandie-Niemen, 13397 Marseille cedex 20, France.

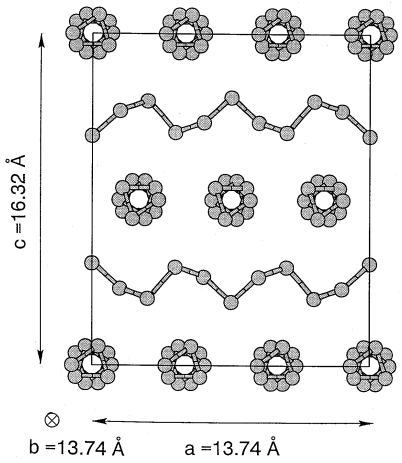

Fig. 2 Lattice structure of $S_{\omega 2}$ as proposed by Tuinstra.[5,10] We represent the helix with 10 atoms per cell along the directions *a* and *b*

Polymeric sulfur is still the subject of experimental work. From X-ray diffraction of powders and FT-IR spectra on commercial polymeric sulfur (Crystex dry-type), Cataldo[1] confirmed the main characteristics of the structures. In particular he found that the commercial product is mainly of the ω_2 type. Olkhov and Jurkowski[7] have made, from mass spectrometry experiments, a thermomechanical analysis of different kinds of sulfurs: the rhombic and polymeric forms. Some years ago, in a laboratory experimental set-up reproducing the industrial process,[8] a refined synthesis of these products has been worked out. It has been observed that $S_{\omega 2}$ was easily synthesized by quenching from the vapour and extraction by CS_2; only traces of $S_{\omega 1}$ were present. A weak heating is sufficient to transform the mixture into a nearly pure $S_{\omega 1}$ phase, as proved by Raman spectra experiments.[8] The difference between the cohesive energies of these two compounds is expected to be small since only the breaking of weak bonds is necessary to convert one structure to the other (see section on Link to Thermodynamic Experiments below). In spite of the refinement of lattice parameters proposed by Michaud,[8a] many features of the structures of $S_{\omega 1}$ and $S_{\omega 2}$ are not fully understood. There are controversies in the determination of interatomic distances from Raman spectra or EXAFS for S_{ω}.[8] Open questions are the following: what are the relative directions of rotation of helices and what is the optimum value of the rotation angle? Are there any relative shifts between parallel helices? Does the unit cell in one helix contain three ($N_{ec} = 3$) or ten ($N_{ec} = 10$) sulfur atoms? A three-atom unit cell has been proposed by Prins *et al.*[9] and Tuinstra[10] for S_{ω}, while a ten-atom pattern has been proposed by Lind and Geller[11] for S_{ψ}, an allotrope close to $S_{\omega 1}$. As other possibilities we could think of 4, 5, 7, 8, *etc.* atoms per elementary cell. The ratios (for 4 and 7) or their inverse (for 5 and 8) of each of these numbers to 3 (or the closest multiple of 3 to it) are greater than the 10/9 ratio, where the number 9 corresponds to 3 times 3 atoms. The 3 and 10 atom structures correspond to the best compromise; the real structure being constrained by covalent distances and valence angles in the chains and the overall steric hindrance between helices. On the other hand, the values of the crystallographic parameters along the helix axis found for these structures also limit the number of atoms in the elementary helical cell. Therefore, in this first study, we decided to limit ourselves to only two cases, that is 3 and 10 atoms per elementary cell. Then, as a last question, what is the influence on the crystalline parameters, when changing from a three-atom unit cell to a ten-atom unit cell for one helix?

No theoretical work has been done so far on 3D polymeric sulfurs. Only a few calculations are related to isolated sulfur chains. A 1D periodic calculation on a helix of sulfur atoms has been carried out some years ago by Springborg and Jones[12] with the local spin density (LSD) approximation of density functional theory (DFT). Then Karpfen[13] ran *ab initio* crystal orbital (CO) calculations while Cui and Kertesz[14] focused on orbital patterns and band structure. Finally, Warren and Gimarc[15] only considered chains through sulfanes to study strain energies in sulfur rings. Here, the size of the unit cells (12 × 10 atoms for $S_{\omega 2}$ in the hypothesis of a cell containing 10 atoms along the *a* and *b* directions) and the number of points necessary to explore the potential surface rule out the use of *ab initio* methods. On the other hand, at the present time, a temperature-dependent simulation on isolated phases, with adjusted potentials, might *be very difficult* to achieve, because of both the complexity of the elementary cells and the nature of bonds requiring an elaborated potential. Therefore a zero-temperature theoretical method treating both covalent and weak interatomic forces, like the one developed in Part I[16] [extended Hückel theory (EHT)[17] for the repulsive energy and a method derived from classical perturbation expansions for the dispersion energy], might bring relevant (although partial) information. A summary of the methods is given in the next section. In previous work on isolated helices,[14,15] it has been shown that semiempirical methods such as the modified neglect of diatomic overlap (MNDO)[18] and EHT may lead to correct results.

Fig. 3 shows the notation used in this work for a single helix, oriented along the *x* axis. The angle θ defines the position of the projection of an atom on the basal plane with respect to the *y* axis. When several helices are considered, the first atom of the first helix defines the basal plane (with $\theta = 0$). For the other helices, assumed to be parallel, the first atom can be out of this basal plane. To define the shift, we only have to consider displacements between 0 and the height of the second atom. In the following we shall use *q*, which is the percentage of the maximum displacement, that is the height *Q* of the second atom. Other notations are obvious: r_{S-S} is the covalent S—S distance, α is the valence angle, β is the dihedral angle and r_h is the radius of the helix.

In Part I, a detailed summary of the methods was first given and the adequate parametrization has been set up. To test the

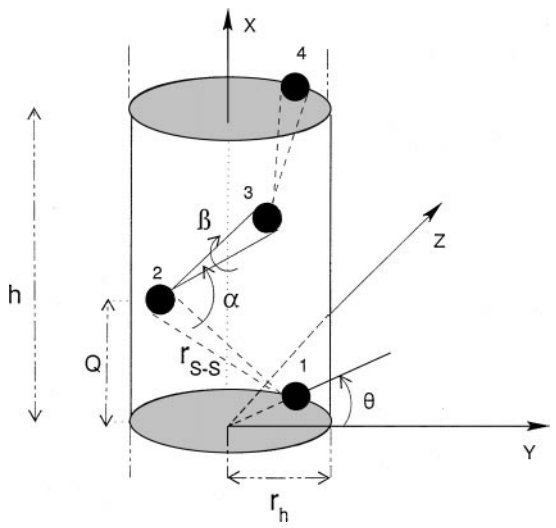

Fig. 3 Elementary unit cell for a 1D helicoidal chain of sulfur oriented to the left. We have represented a three-atom unit cell ($N_{ec} = 3$); atom 4 is obtained from atom 1 by a translation of length *h*. (The height *h* will exactly correspond to the proposed experimental crystallographic parameter *c* in the $S_{\omega 1}$ case with $N_{ec} = 3$, while its value is 3*c* in the $N_{ec} = 10$ case. Likewise, in the $S_{\omega 2}$ case, *h* is linked to the crystallographic parameters *a* or *b*, depending on the N_{ec} value.) The projection of atoms 2 and 3 are rotated by $2\pi/N_{ec}$ around the *x* axis and their distances to the basal plane are a multiple of h/N_{ec}. The angles α and β are the angles between two neighbouring covalent bonds and the torsion angle around that bond

method we first chose the well-known S_α structure, made of S_8 molecules in weak interactions. Though not directly involved in the weak intermolecular energy calculations, we checked in a preliminary calculation on S_8 that EHT was able in that case to reproduce correctly its structure (the errors were only 2, 4 and 6% on the covalent distances, the valence angles and the dihedral angles, respectively). For the crystal, we have found the correct *c* crystallographic parameter and errors lower than 4 and 6% for the *a* and *b* crystallographic parameters, respectively. Moreover, the enthalpy of sublimation has been determined and the difference with the experimental value fell within the error range of the mass spectrometer measurement, that is 5%. Then, in prevision to a study of ω-allotropes, we considered two helices in interaction (1D calculations) but only in one configuration ($[N_{ec} = 3, rr]$ in our notation) as a further test. We suggested in this preliminary calculation that the angle θ and the shift q may be determined from the repulsive energy only since the total interaction energy contour map and that obtained by only considering the repulsive energy (as functions of the shift and the rotation angle of one helix relative to the second) have very similar shapes. The value of the van der Waals radius of sulfur only differed by 0.6% from the experimental one. From the interhelix distance and the total interaction energy found in this simple case, we concluded that it would be reasonable to treat more realistic 3D helical structures with this method.

The scope of this second part is to bring some new insights on the structures of ω-type sulfurs. In this work we have also estimated the enthalpy of sublimation and compared it to the experimental value obtained in a mass spectrometer coupled with a Knudsen effusion cell.[19] Even limiting ourselves to the structures given in Fig. 1 and 2, there are many degrees of freedom to take into account in order to approach the realistic 3D structures. Our strategy was to proceed step-by-step. We have first optimized the relative geometry between two helices in one dimension but now in all cases corresponding to our model. Then, 2D calculations introduce the environment resulting from this new periodicity and the contribution of non-neighbouring helices. Finally, taking into account 1D and 2D results, the lowest energy for 3D structures is obtained in only a few calculations. This will be the structure of this paper, with a first section briefly recalling the theoretical methods. A second section is devoted to 1D and 2D calculations which, though unphysical, are easy to run and are used to set up the framework for the real 3D calculations of the next sections. Finally, a discussion concerning thermodynamic data is the scope of the last section.

Theoretical Methods

For large systems, a simplified formulation for the interaction potential between the two systems is needed. For weakly polar or nonpolar systems this potential reduces to only a short-range repulsive part and a long-range dispersion part. Let us briefly recall the main points.

Repulsive and dispersion energies

In the case of large systems, EHT[17] implemented on crystalline structures[20] has proven to give the correct repulsive energies for the description of the physisorption of alkanes on graphite[21] and for the adsorption of argon in silicalite zeolite ZSM-5.[22] More recently (in Part I[16]) we have studied the structure and the thermochemical description of α-sulfur with the set of parameters used in this study. Periodic EHT equations have been widely developed and discussed in the literature. Atoms from the unit cells are described by valence Slater-type orbitals. Translation vectors apply to define the periodic system. Then, a set of atomic Bloch sums $\phi_j(\boldsymbol{k})$, where $\boldsymbol{k}$ is a vector in the reciprocal space, is constructed. The crystal orbitals $\psi_j(\boldsymbol{k})$ are linear combinations of Bloch sums, whose coefficients are obtained from the variational theorem. The application of this variational theorem for each $\boldsymbol{k}$ point leads to the secular determinant:

$$|H_{\mu\nu}(\boldsymbol{k}) - e(\boldsymbol{k})S_{\mu\nu}(\boldsymbol{k})| = 0 \quad (1)$$

where the energy integral $H_{\mu\nu}(\boldsymbol{k})$, the overlap integral $S_{\mu\nu}(\boldsymbol{k})$ and energies $e(\boldsymbol{k})$ are defined in terms of Bloch functions. The overlap integral $S_{\mu\nu}(\boldsymbol{k})$ is directly expanded in terms of basic overlap integrals between atomic orbitals $S_{\mu\nu}$; it is modulated by a phase-dependent term. *In fine* the energy integrals $H_{\mu\nu}$ are expressed in terms of overlap integrals and the atomic energy levels $H_{\mu\mu}$ and $H_{\nu\nu}$, according to the weighted formula.[23] Resolution of eqn. (1) is carried out for a set of representative points in a reduced part of the Brillouin zone and the energy is averaged over these points. The choice of the number of $\boldsymbol{k}$ points,[24] for the sampling of the reduced Brillouin zone, has been discussed in Part I.[16]

Concerning the second part of the energy, application of time-dependent perturbation theory leads to a dispersion multipole expansion, which in the case of two-body terms, is expressed as:

$$u_d^{AB}(R) = -[C_6^{AB}R^{-6} + C_8^{AB}R^{-8} + C_{10}^{AB}R^{-10} + \cdots] \quad (2)$$

where the *C*s are coefficients describing multipole interactions and *R* represents distances. These coefficients are linear combinations of basic two-body coefficients whose general formulation in atomic units is:

$$C^{AB}(l_1, l_2) = \frac{(2l_1 + 2l_2)!}{4(2l_1)!(2l_2)!} \frac{\eta_{l_1}^A \eta_{l_2}^B}{\eta_{l_1}^A + \eta_{l_2}^B} \alpha_{l_1}^A(0)\alpha_{l_2}^B(0) \quad (3)$$

where l_1 and l_2 equal 1, 2, ... for a dipole, a quadrupole, *etc.*, α_l is the static *l*th pole polarizability and η_l is an average *l*th pole transition energy for each interacting atomic species A and B.[25] Finally, it has been shown[25,26] that the coefficients C^{AB} may all be expanded as a function of two parameters: the effective number of electrons N_{eff}^A for the species A and the in-framework dipolar polarizability α_1^A (and the same for the species B). In general, polarizabilities are known for only a few solid state systems and the empirical evaluation of these two parameters is discussed below in the parametrization section. Moreover, in order to take into account the fact that overlap between electron clouds cannot be neglected at short-range separations, that is around the equilibrium distances, a *damped* multipole expansion was introduced.[27] Eqn. (2) is modified by the introduction of damping functions f_{2n} multiplying the C_{2n} coefficients. Finally, perturbation theory up to third- and fourth-order is necessary to obtain three-body dispersion terms involving triplets of species A, B and C. Similar equations to those for two-body interactions can be found elsewhere.[25] The sign of these three-body terms depends on the geometrical configuration since such triplets are both distance- and angle-dependent. Their relative balance and therefore the final sign of the three-body term is in general unpredictable but its importance has been emphasized in some test calculations in Part I. In the case of two helices in interaction, also in Part I, we have calculated the relative contributions of the R^{-6} and R^{-8} terms. The R^{-8} term is lower, in absolute value, than the three-body term, at least in the region where the three-body term decreases with *R*. This clearly means that the introduction of C_{10}, and higher, coefficients and terms is not necessary. We have also checked that the introduction of damping functions in the calculation of three-body terms is not important.

Parametrization

The retained parameters for the repulsive part (EHT calculations) are equal to: $\zeta_s = \zeta_p = 1.817$, $H_{ss} = -20.0$ eV and $H_{pp} = -13.3$ eV. They have been tested on α-sulfur in Part I.[16]

For dispersion equations, two key parameters, N_{eff} and α_1,

are sufficient to determine all C_{2n} and three-body coefficients. For neutral sulfur N_{eff}^{S} has been estimated[16] at 4.93. In-framework ionic or atomic dipole polarizabilities can be derived by combining the general relaxation theory of Auger spectroscopy[28] with Moretti's electrostatic model.[29] In the case of α-sulfur, the S dipole polarizability was estimated at 5.39 Å^3 as shown in Part I of this study.[16] The S polarizability in polymerized sulfur is assumed to be identical to that found for α-sulfur since the local environment of S atoms is the same in both structures.

Interaction Energy of Sulfur Helices in Low-dimension Systems

Structure of one isolated helix

It is easy to perform accurate *ab initio* calculations on one isolated helix with either three or ten sulfur atoms in its elementary cell. These cells give valence angles α close to 109° and dihedral angles β close to 90° (*gauche* effect) as found for example in an *ab initio* calculation on HSSH. This means that S—H bonds (S—S bonds in sulfur helices) conjugate to lone pairs of neighbouring atoms rather than to neighbouring bonds. Using EHT for the repulsive part of the chain-chain interaction energy, we also have to search for the lowest energy structures. In Table 1 are listed the optimized structures obtained either directly or by extrapolation from crystalline parameters by using different procedures: LSD,[12] CO,[13] SCF[30] and EHT (this work).

As the isolated helix is a model, the 'experimental values' result from a compromise between experiments on S_ω and on S_ψ (an allotrope also made of helical chains but with no well-defined cell length along the helix axis). Since the interatomic distances deduced from Raman spectra (≈2.05 Å) or EXAFS (≈2.15–2.18 Å) are quite different[8] for S_ω, we focused on the well-determined values proposed by Tuinstra[10] and Lind and Geller[11] for S_ψ (2.07 Å). This value, associated with $N_{ec} = 3$ and the crystallographic parameter c, that is h in our notation for one isolated helix (see Fig. 3 caption for explanations about h and the link to the crystallographic parameters), allow us to determine α, β and r_h. For $N_{ec} = 10$, we chose for h three times the experimental value h_{exp} associated with $N_{ec} = 3$. Then, the other parameters are straightforwardly determined. Optimal geometries for the helix are reported in Table 1. In the case of the *ab initio* cluster calculation,[30] we report the result for the central part of the 11-atom cluster. Optimized EHT results compare well with others. The r_{S-S} distance is more reasonable than that from the DFT calculation. The cell length is slightly too large as in other calculations, except for the CO value, which is rather good. In fact, in our study, which focuses on the relation between different helices, the description of the covalent bonds of the helix itself is not the most important part. We chose to impose the geometries deduced from available experimental data.

Regarding EHT dissociation energies, the lowest values are: $E_{(3)} = -3.692$ eV atom^{-1} for $N_{ec} = 3$ and $E_{(10)} = -3.675$ eV atom^{-1} for $N_{ec} = 10$. The structure with $N_{ec} = 3$ is more stable than that with $N_{ec} = 10$ [$\Delta E_{3\text{-}10} = -0.017$ eV atom^{-1} $= -1.6$ kJ (mol S)$^{-1}$]. In this paper we are mainly interested by weak interactions and energies between helices. However, we shall consider in our discussion the influence of the $\Delta E_{3\text{-}10}$ difference in comparing structures.

Table 1 Optimized structure of one isolated helix of sulfur atoms obtained from different theoretical methods. See text and Fig. 1 for notations and Fig. 3 caption for the link between h and the crystallographic parameters

Method	r_{S-S}/Å	α/°	β/°	r_h/Å	h/Å
3 atoms per cell					
EHT	2.12	110.9	105.3	0.80	4.81
3D Expt. ($S_{\omega 1}$)	2.07	108.5	103.9	0.81	4.58
10 atoms per cell					
LSD[12]	2.23	109.0	86.5	1.00	15.49
CO[13]	2.08	105.1	79.7	1.01	13.37
SCF(cluster)[30]	2.07	111.0	89.2	0.89	14.90
EHT	2.09	111.4	89.3	0.90	15.00
3D Expt. ($S_{\omega 1}$)	2.07	105.4	84.7	0.96	13.74

Interaction of two 1D helices

All the geometrical parameters important for the cohesion of the crystal (θ, q, the number of atoms in the elementary cell, N_{ec}, and the direction of rotation of helices) can be easily varied on this simple system. First, we will consider their influence on both the repulsive energy and the total energy at a fixed interchain distance, R. We chose $R = 4.5$ Å as a mean 'experimental value' since it is close to the a value of $S_{\omega 1}$. Then R will be varied in order to get the cohesion of this 1D system.

In Fig. 4, the repulsive energy as a function of θ is shown for typical values of q, in the case [$N_{ec} = 10$, rl]. The lowest energies (≈0.059 eV atom^{-1}) are obtained for $q = 1/2$, $\theta = 18°$ and 90°. Below $\theta = 120°$ there is a low-energy region where it might be easy to change conformation. For $\theta = 240°$ (rl case) or $\theta = 120°$ (rr case), the energy is independent of q. The general shape of the curves for other cases is the same. The energy minima are located at low θ (rl case) or at high θ (rr case) values. The energy minima are found for the displacement $q = 1/2$. In the case [$N_{ec} = 10$, rr], the energy minimum is unique (at $\theta = 306°$) but, as in other cases, all energy curves corresponding to various q values are close together in that region. The values of q and θ leading to repulsive energy minima are gathered in Table 2. Up to now, the case [$N_{ec} = 3$, rr] is the less repulsive and therefore the most stable.

We have now to include the dispersion energy. In Fig. 5, we have plotted the two separate contributions (repulsion and dispersion) and the total energy over the whole range of θ for $N_{ec} = 10$, disrotatory helices and $q = 1/2$ (the lowest curves in the low-energy regions in all cases). The shape of the total energy is very similar to that of the repulsion energy. However, the total energy changes of sign and the cohesion of the structure appear in the low-energy region. Above $\theta = 120°$

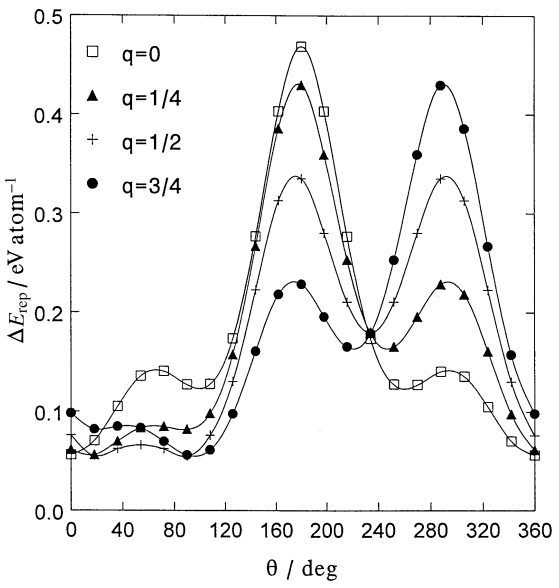

Fig. 4 Repulsive interaction energy between two infinite disrotatory (rl) 1D helices (10 atoms per cell) of sulfur atoms, as a function of θ, for different representative q values

Table 2 Comparison of the total interaction energy minima between two infinite 1D helices

	$N_{ec} = 3$, *rr*	$N_{ec} = 3$, *rl*	$N_{ec} = 10$, *rr*	$N_{ec} = 10$, *rl*
q	1/2	1/2	1/2	1/2
θ/°	260–340	20–100	306	18–90
ΔE_{rep}/eV atom^{-1}	0.058	0.054	0.088	0.084
R_{min}/Å	4.26	4.29	4.40	4.39
$\Delta E_{2\text{-body}}$/eV atom^{-1}	−0.138	−0.132	−0.154	−0.154
$\Delta E_{3\text{-body}}$/eV atom^{-1}	−0.031	−0.030	−0.055	−0.052
ΔE_{min}/eV atom^{-1}	−0.111	−0.108	−0.121	−0.122

the repulsion part is so strong that the two helices remain separated. Before proceeding to higher dimension crystals, we have to verify that the values of q and θ determined from these 1D calculations are really the ones giving the lowest energy (or very close to) structures. In the low-energy region (θ = 0–108°) we obtain the same energy curves as in Fig. 5 for different values of q. Not only are the curves (not shown) corresponding to the total interaction energy in the same order as those corresponding to the repulsive energy, but also the lowest one ($q = 1/2$) is more separate from the three others than in the repulsive case. Therefore, it seems quite legitimate to adopt the θ values determined, at a given value of q, *from the repulsive energy variation only*.

In Fig. 6 the partitioning of the total interaction energy is analysed for disrotatory helices with $N_{ec} = 10$. We adopted the optimized values, $q = 1/2$ and $\theta = 18°$, determined above. The two-body dispersion part includes inverse powers of six and eight of the interchain interatomic distances and it is the importance of three-body terms that has to be noticed here. This contribution is larger than in the $N_{ec} = 3$ case (shown on Fig. 7 in Part I). Without these terms the minimum in the total interaction energy occurs at $R_{min} = 4.49$ Å with $\Delta E_{min} = -0.073$ eV atom^{-1}. At this point, in absolute values, the three-body term is equal to approximately 3/4 of the repulsive energy and 1/3 of the two-body part. Adding the three-body term, the minimum is pushed towards lower values of R: $R_{min} = 4.39$ Å and $\Delta E_{min} = -0.122$ eV atom^{-1}.

Our results for the interaction of the two 1D helices are summarized in Table 2. Let us note that the ΔE_{rep} values given in Table 2 are different from the values discussed above since they correspond to the optimized value of R. For the values of q and θ used, the main difference lies rather in the number of atoms in the elementary cell than in the relative direction of rotation of the helices. The ten-atom elementary cell seems to be the most stable, but it is still hazardous to choose between the *rr* and the *rl* relative directions of rotation of helices.

We also have to emphasize two points. (*i*) Looking at the repulsive contributions only, for $R = 4.5$ Å, a value close to the R_{min} values of Table 2, we would have concluded that the most stable structure is that corresponding to the [$N_{ec} = 3$, *rr*] case. When the dispersion terms are included, we conclude that the interactions are more favourable in the case where $N_{ec} = 10$, more precisely for the disrotatory mode, not on the sole argument of the slight energy difference, but also on the larger domain of θ where the energy is close to the minimum. Therefore, the consideration of dispersion energy changes the configurations and some relative conformations of helices for the most stable systems. (*ii*) When adding the $\Delta E_{3\text{-}10}$ (covalent) term the new energies for the structures given in Table 2 from left to right read: −3.803, −3.800, −3.796 and −3.797 eV atom^{-1}, respectively. The order has been reversed and the [$N_{ec} = 3$, *rr*] structure is the most stable. However, caution must be taken since the energy values are small.

Interaction of 2D-structures of parallel helices

Adding one dimension to our system means that we repeat along the y axis (Fig. 3) the two infinite 1D helices (the unit cell contains two helices; one is shifted relative to the other). Each helix has now two neighbouring helices. Such a system is still relatively small and allows q and θ to be varied.

In Fig. 7, we plot, for all values of q, the case [$N_{ec} = 10$, *rr*]. This is an example of curves with a unique energy minimum (at $\theta = 306°$), typical of such configurations, as already mentioned in the 1D case. The energies per atom are

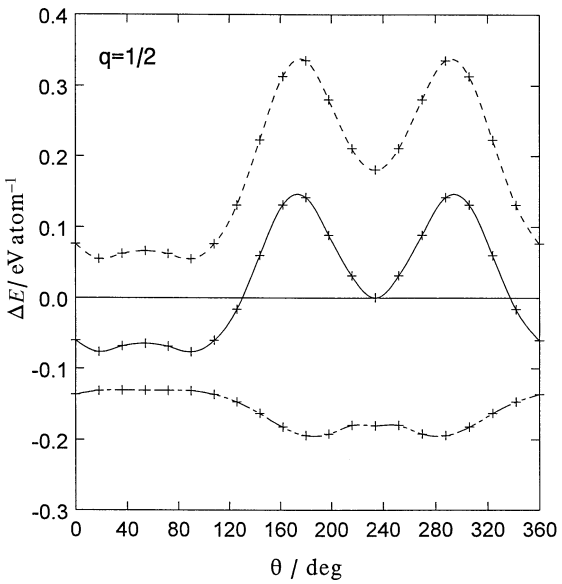

Fig. 5 Partitioning of the interaction energy between two infinite disrotatory 1D helices (10 atoms per cell) of sulfur atoms and $q = 1/2$, as a function of θ. Curves are as follows: (——) repulsion energy, (– ·· – ··) dispersion energy, (——) total energy

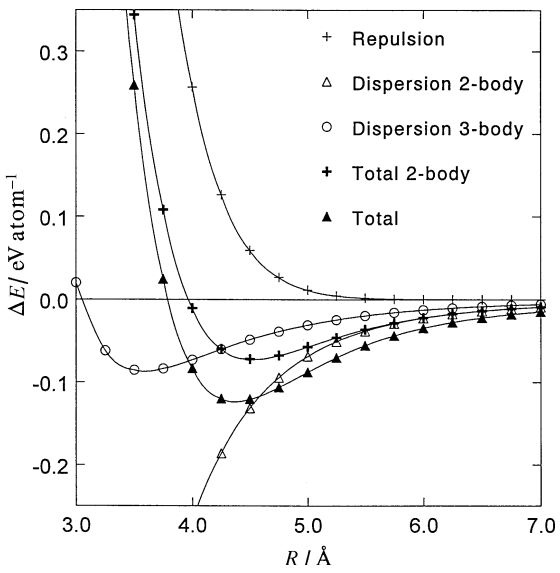

Fig. 6 Partitioning of the interaction energy between two infinite disrotatory 1D helices (10 atoms per cell) of sulfur atoms *versus* the interchain distance ($q = 1/2$, $\theta = 18°$)

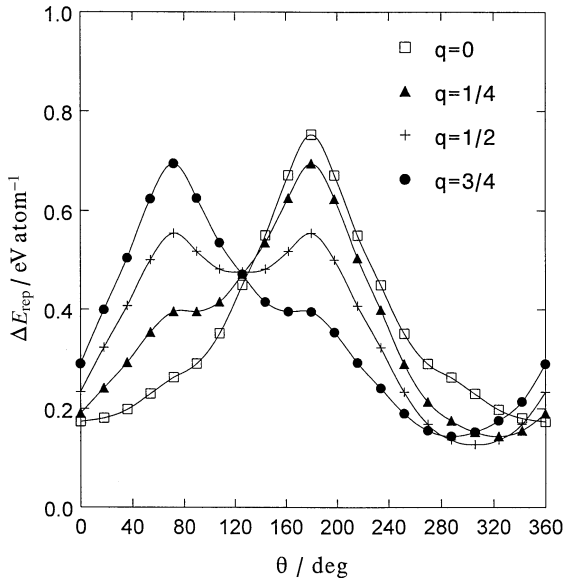

Fig. 7 Repulsive interaction energy between an alignment (2D) of infinite conrotatory helices (10 atoms per cell) of sulfur atoms, as a function of θ, for different values of q

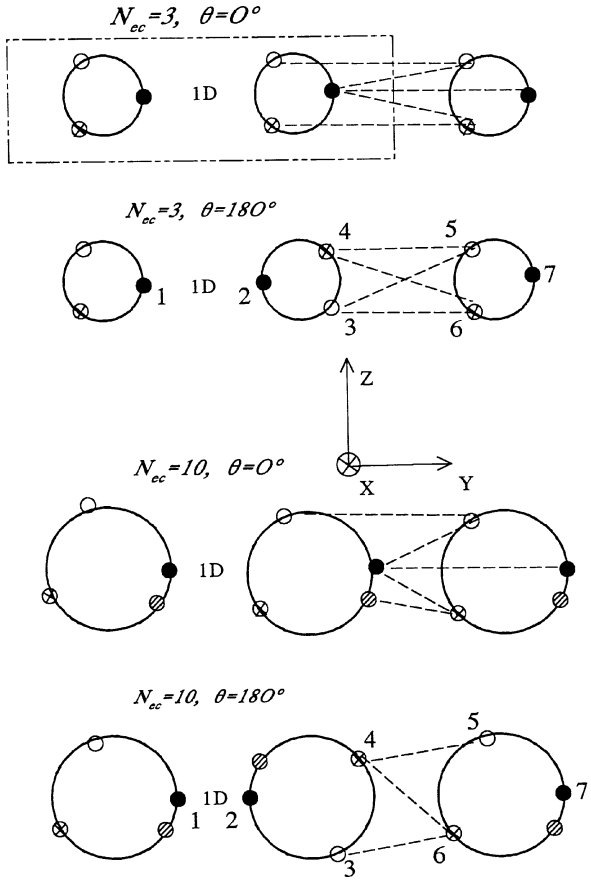

Fig. 8 Additional interactions brought about by the consideration of 2D structures instead of 1D structures

slightly larger in the 2D case than in the 1D case. In the extreme case for $\theta = 0°$, these are twice as large as in the 1D case. In Fig. 8, we have drawn the projections of helices for two typical cases of θ. For the sake of clarity, the q parameter has been set equal to zero and helices are conrotatory in the *ll* mode. The atoms represented by a full black circle are in the basal plane. The height of other atoms increases when rotating in the counter-clockwise direction. The elementary cell is shown in a rectangle. Increasing the dimension to two implies to consider as new all interactions arising on one side of the elementary cell only. For $\theta = 0°$, in both cases, the new interactions are exactly the same as the 1D interactions. Therefore, we may expect a doubling of the interaction energy, which is effectively observed. For $\theta = 180°$, the strong interaction between the atoms labelled 1 and 2 in the 1D system is not multiplied by two when considering the 2D system. Indeed, we have $r_{27} \gg r_{12}$ and the interaction between atoms 2 and 7 is negligible. This is partly compensated by the couples of atoms 4 and 5 on the one hand, and 3 and 6 on the other hand, which are now closer than in the $\theta = 0°$ case. Moreover, because of both the different helix radii and the position of atoms 4 and 5 (and 3 and 6) on the helix, the interactions between the atoms 4–6, 4–5 and 3–6 are much stronger for $N_{ec} = 10$ than for $N_{ec} = 3$. The same type of sketches were successfully used in Part I. Curves corresponding to other cases, [$N_{ec} = 3$, *rr*] and [$N_{ec} = 10$, *rl*], are also quite comparable to the 1D cases, and deserve the same comments.

The results for 2D arrangements of parallel helical chains are given in Table 3. For the case [$N_{ec} = 10$, *rl*], a little ambiguity appears. In the low-energy region, all q values give comparable minima of the repulsive energy (in eV atom^{-1}): $q = 0$, 0.112, $q = 1/4$, 0.113; $q = 1/2$, 0.119; $q = 3/4$, 0.113, at the same interchain distance $R = 4.5$ Å that used as a reference in the 1D case. After taking into account the dispersion energy, it has been clearly shown that the total energy has a minimum value for $q = 1/2$ and this is the final value given in Table 3. Two main conclusions can be drawn from these 2D calculations. First, the lowest energy structure differs from that obtained from the 1D case. Here the [$N_{ec} = 3$, *rl*] case corresponds to the lowest energy, but the interchain distance has shortened. Secondly, the repulsive energy alone is sufficient to determine the lowest energy structure in terms of q and θ. Indeed, the lowest repulsive energy (in eV atom^{-1}) for each case and for $R = 4.5$ Å are: [$N_{ec} = 3$, *rr*, $q = 1/2$], 0.058; [$N_{ec} = 3$, *rl*, $q = 1/2$], 0.042; [$N_{ec} = 10$, *rr*, $q = 1/2$], 0.130; [$N_{ec} = 10$, *rl*, $q = 0$], 0.112. The slight controversy in the last case has been discussed above and has no influence on the final determination of the lowest energy 2D case: [$N_{ec} = 3$, *rl*]. However, we must be aware of such inversions of stabilities depending on q values for lowest energy regions in real 3D systems. Finally, the addition of ΔE_{3-10} increases the energy difference between the $N_{ec} = 3$ and $N_{ec} = 10$ structures. The two structures corresponding to $N_{ec} = 3$ have a lower energy than the two structures with $N_{ec} = 10$.

Table 3 Partitioning of the total interaction energy of 2D systems of parallel helical chains of sulfur atoms

	$N_{ec} = 3$, *rr*	$N_{ec} = 3$, *rl*	$N_{ec} = 10$, *rr*	$N_{ec} = 10$, *rl*
q	1/2	1/2	1/2	1/2
θ/°	300	60	306	18–90
ΔE_{rep}/eV atom^{-1}	0.144	0.202	0.189	0.180
R_{min}/Å	4.23	3.98	4.38	4.37
$\Delta E_{2\text{-body}}$/eV atom^{-1}	−0.299	−0.370	−0.319	−0.318
$\Delta E_{3\text{-body}}$/eV atom^{-1}	−0.102	−0.090	−0.116	−0.110
ΔE_{min}/eV atom^{-1}	−0.240	−0.259	−0.250	−0.250

3D Systems

Lowest energy structures of ω_1-type 3D crystals

As outlined in the introduction we limited our scope to a discussion of Tuinstra's proposals for structures. Therefore, we mainly considered as the basic structure the one shown in Fig. 1, that is a structure where we have conrotatory helices along zig-zag arrangements: helices **A**, **C** and their *b*-translated helices on the one hand, and helices **B**, **D** and their *b*-translated helices on the other hand. From 1D and 2D calculations we have found that an *rl* arrangement leads to a lower energy than an *rr* one. Here it is straightforward to see that we cannot have the *rl* arrangement in all directions. Therefore, we decided to consider two structural types. First, the structure proposed by Tuinstra, described above, and denoted *rlrl* with respect to helices **A**, **B**, **C** and **D**, respectively. Secondly, a structure with all helices being conrotatory, such as *rrrr*, as the energy difference was relatively small in the 1D and 2D results.

In the first case, let us note that our 1D (with caution) and 2D results are consistent with Tuinstra's proposals since the arrangement *rl* is much more favourable in the *a* direction (**AB** or **CD** in Fig. 1) than in the *b* direction. Indeed, for the assumed equilibrium geometry, helices are closer in this direction than in the other and this alternance of rotation direction might bring more cohesive energy than the *rr* arrangement (at least this was the case for 2D structures). Now, considering q and θ values, the direct application of 1D and 2D results to *all* helices is impossible to achieve, as it was the case for the relative directions of rotation discussed above. To be consistent with previous assumptions we will assume that in zig-zag arrangements of conrotatory helices, the structural parameters θ and q will be the same. We also keep this definition in the study of the second structural type: *rrrr*. Therefore, as for lower dimension cases, one value of θ and one value of q will be sufficient to describe the structure in the **BD** plane (since in all the **AC**-type planes we take $\theta = 0°$ and $q = 0$ as the origins).

As in 1D and 2D calculations, let us first look at the variations of the repulsive energy as a function of θ and q, considering the 'experimental values': $a = 9.02$ Å, $b = 8.32$ Å. We must expect differences with the preceding results since, for example, in the dispersion part of the energy, it is necessary to consider fourteen helices surrounding a central one (instead of four in the 2D case) to achieve good convergency of the energy. In Fig. 9, the curves for the case [$N_{ec} = 3$, *rlrl*] are plotted *versus* the angle θ. The general shapes are still the same as in previous low-dimension cases. Moreover, relative to 1D values, apart from the values of θ close to zero where the repulsive energy is nearly tripled, the remaining parts, although slightly increased, are of the same order. On the other hand, for *rrrr* configurations, the similarity between the three types of curves (1D, 2D and 3D-ω_1) is still more pronounced and all values are practically the triple of the 1D values. Our rough reasoning made from schemes in Fig. 8 still applies to this 3D structure. All arguments given for *rrrr* structures also apply to *rlrl* structures. The lowest repulsive

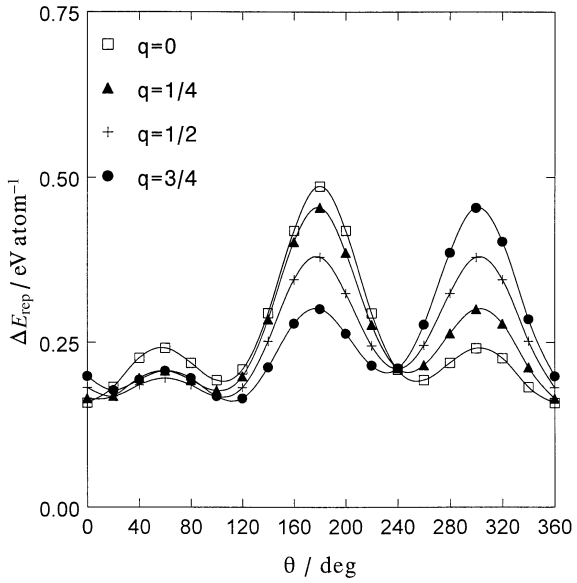

Fig. 9 Repulsive interaction energy between helices [$N_{ec} = 3$, *rlrl*] in ω_1-sulfur, as a function of θ, for different values of q

energies (at experimental structural crystal parameters) are given in Table 4. The slight controversy found for 2D systems, that is the inversion between the $q = 0$ and $q = 1/2$ cases as the lowest structures, by introduction of the dispersion forces, is still present in *rlrl* structures of ω_1-sulfur. As previously, the $q = 1/2$ structure becomes the most stable after introduction of the dispersion.

All final results are gathered in Table 4. It is clear that the most stable structure is that corresponding to an elementary cell of four helices with three atoms per helix and zig-zag arrangements of disrotatory helices. The crystalline parameters a and b are slightly higher than the expected 'experimental values'. As in lower dimension cases, the introduction of the dispersion part of the energy has decreased the difference energy between structures relative to the repulsive energy values. But the relative orders were not changed. The addition of the term $\Delta E_{3\text{-}10}$ does not change these conclusions.

Structures of ω_2-type sulfur crystals

The structure proposed by Tuinstra for this type of crystal is much more complicated than the structure of $S_{\omega 1}$. From Fig. 2, we see that the proposed crystalline cell is a succession of planes containing parallel helices. From one plane to the following, the axes of the helices are perpendicular. Even with such a well-defined general structure, the number of possible conformations is so large that we have only considered the most stable ones. Concerning the number of $\boldsymbol{k}$ points to be used, we followed the same procedure.[31]

Taking advantage of our preceding results, we may first assume that in a given plane all helices are conrotatory, as

Table 4 Lowest repulsive interaction energies and lowest total interaction energies and structures of ω_1-sulfur

	$N_{ec} = 3$, *rrrr*	$N_{ec} = 3$, *rlrl*	$N_{ec} = 10$, *rrrr*	$N_{ec} = 10$, *rlrl*
q	1/2	1/2	1/2	1/2
θ/°	300	20	306	108
ΔE_{rep}[a]/eV atom^{-1}	0.110	0.169	0.265	0.369
a_{min}/Å	8.75	9.50	9.60	9.71
b_{min}/Å	7.92	8.99	8.70	9.25
ΔE_{min}/eV atom^{-1}	−0.268	−0.287	−0.223	−0.248

[a] At experimental structural crystal parameters.

suggested by Tuinstra. Until now, a direction of rotation (*r* or *l*) was associated to *one helix only*. In the ω_2-crystal it will be associated to *all helices in a given plane*; then capital letters are used. The first structure we have to consider is the *RLRL* one since we have four planes involved in the construction of the crystalline cell. However, we must also consider as possible structures those obtained by considering planes of helices rotating in other directions. Logically we chose to study *RRLL* and *RRRR* arrangements. Now, we have to introduce the variations as a function of q and θ. We limited ourselves to the cases where we have the same values of q and θ in two successive planes with, as previously and by definition, $q = 0$ and $\theta = 0°$ in the first two planes. This looks like an acceptable approximation as the axes of two helices in these planes respectively are perpendicular so that the relative influences of θ and q values are much less important than in the case where the axes are parallel (since in this case only small parts of the two helices are close together). Of course we also have to consider the two cases $N_{ec} = 3$ and $N_{ec} = 10$. The variations of the repulsive energy for all cases considered are given in Table 5. They have been evaluated at an interplane distance of $R = 4.08$ Å. This value corresponds to a quarter of the 'experimental value' of *c* (see Fig. 2).

From the repulsive energy only, the lowest energy structures might be of the *RRLL* type with $q = 3/4$ or 1/2 for $N_{ec} = 3$. Some test calculations were also carried out for $q = 1/4$ and 3/4 in the case $N_{ec} = 10$. We found a different behaviour of the energy as a function of q than in the $N_{ec} = 3$ case. For example, in the *RRRR* configuration with $q = 1/4$, the lowest energy value (0.661 eV atom^{-1}) was reached for $\theta = 72°$. This energy is intermediate between the $q = 0$ and $q = 1/2$ cases. But we know that we have to take care of possible inversions of stability appearing with the introduction of the dispersion energy. In order to analyse such effects, we also calculated the total energy for some structures that are not the lowest in energy in Table 5. In this complicated structure, the convergence in the calculation of the dispersion energy was only achieved by considering 14 helices surrounding a central one for $N_{ec} = 3$ and 36 helices for $N_{ec} = 10$.

In Table 6 we give the total minimum interaction energies in the two cases $N_{ec} = 3$ and $N_{ec} = 10$ for some selected low-energy structures. Some other cases were found not to be competitive as the lowest energy structures. For example: [$N_{ec} = 3$, *RRRR*, $q = 1/2$, $\theta = 40°$]: $R_{min} = 4.33$ Å and $\Delta E_{min} = -0.206$ eV atom^{-1} and [$N_{ec} = 3$, *RLRL*, $q = 1/2$, $\theta = 320°$]: $R_{min} = 4.67$ Å and $\Delta E_{min} = -0.165$ eV atom^{-1}.

Table 5 Lowest repulsive interaction energies of typical ω_2 structures at experimental structural crystal parameters

	q	*RRRR*	*RLRL*	*RRLL*
$N_{ec} = 3$				
θ/°	0	100	160	260
ΔE_{rep}/eV atom^{-1}		0.270	0.280	0.235
θ/°	1/4	40	220	260
ΔE_{rep}/eV atom^{-1}		0.279	0.360	0.194
θ/°	1/2	40	320	280
ΔE_{rep}/eV atom^{-1}		0.231	0.345	0.177
θ/°	3/4	40	320	20
ΔE_{rep}/eV atom^{-1}		0.213	0.289	0.175
$N_{ec} = 10$				
θ/°	0	90	90–270	126–306
ΔE_{rep}/eV atom^{-1}		0.659	0.929	0.928
θ/°	1/4	72	108	36
ΔE_{rep}/eV atom^{-1}		0.661	0.851	0.842
θ/°	1/2	72	288	324
ΔE_{rep}/eV atom^{-1}		0.666	0.881	0.622
θ/°	3/4	72	54	162
ΔE_{rep}/eV atom^{-1}		0.651	0.728	0.989

Table 6 Lowest total interaction energies of typical ω_2 structures

N_{ec}	q	θ/°	Configuration	R_{min}/Å	ΔE_{min}/eV atom^{-1}
3	0	260	*RRLL*	4.27	−0.222
	1/4	260	*RRLL*	4.07	−0.259
	1/2	280	*RRLL*	3.90	−0.292
	3/4	20	*RRLL*	4.16	−0.214
10	0	90	*RRRR*	4.83	−0.216
	1/4	72	*RRRR*	4.89	−0.225
	1/2	324	*RRLL*	4.67	−0.239
	3/4	72	*RRRR*	4.81	−0.202

The lowest energy is obtained for the structural case: [$N_{ec} = 3$, *RRLL*, $q = 1/2$; $\theta = 280°$]. The repulsive energy was the lowest for $q = 3/4$ but taking into account the dispersion part has definitely led to the $q = 1/2$ structure being the most stable. The *RLRL* structure is definitely not the most stable. As for ω_1, the addition of ΔE_{3-10} does not change these conclusions.

Link to Thermodynamic Experiments

Sublimation enthalpy differences have been obtained in a mass spectrometer coupled with a Knudsen effusion cell.[19] These experiments investigate the stability of the gaseous clusters in equilibrium with the solid. Taking S_8 as the reference, an enthalpy of sublimation equal to $\Delta H_{sub} = 142 \pm 5$ kJ mol^{-1} is obtained at 298 K and 1 atm. A Hess diagram connecting our calculations (at 0 K) to experiments is visualized in Fig. 10. In our work we have calculated ΔE_1 (so-called in Fig. 10) for both allotropes (ω_1 and ω_2) and found that the most stable structure was that corresponding to $N_{ec} = 3$. The determination of ΔE_2 would allow us to obtain $\Delta E_{sub}^{0\,K}$ and then the experimental value by adding the integral of ΔC_p, the difference between molar heat capacities issued from low temperature adiabatic calorimetry experiments.[32] The determination of ΔE_2, since it involves the breaking and the building of strong covalent bonds, would require us to go beyond our semiempirical approach. Therefore, we can try to evaluate ΔE_2 independently, from an elaborate *ab initio* calculation. The CRYSTAL 92 program[33] treats infinite systems at the Hartree–Fock level. It is well-suited in this case since we have an infinite helix on the left-hand side of the reaction. The electronic correlation is not taken into account but we saw in Table 1 that even LSD results, including one part of the correlation energy, were not very convincing for the determination of structural parameters of one isolated helix. In CRYSTAL 92, we used a 6-21G* atomic basis set with one d polarization function.[34] To avoid spurious effects, because of the neglect of the electronic correlation, we used 'experimental' distances and angles: a D_{4d} crown-shaped structure for S_8 and the values, deduced from ω-sulfur experiments, discussed in the

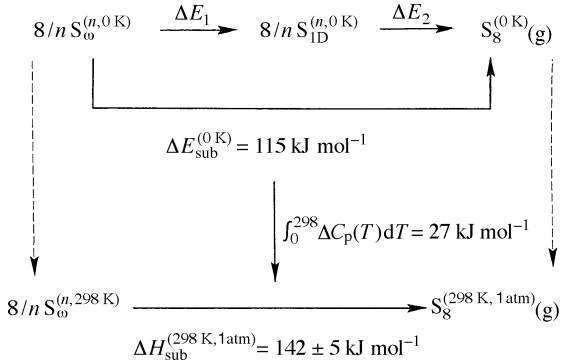

Fig. 10 Hess diagram linking solid and vapour through theory and experiments ($n \equiv N_{ec}$)

beginning of this paper. From total energy values,[35] the energy of the reaction is equal to: $\Delta E_2 = E(S_8) - 8/3\ E(S_{3(\infty)}) = -92.9$ kJ (mol S_8)$^{-1}$. Converting everything into kJ mol^{-1}, we have from Table 4 $\Delta E_1(\omega_1) = 221.5$ kJ mol^{-1} and from Table 6 $\Delta E_1(\omega_2) = 225.4$ kJ mol^{-1} (signs have been changed in order to be consistent with thermodynamics conventions). Finally, we obtain $\Delta E^{0\,K}_{sub}(\omega_1) = 128.6$ kJ mol^{-1}, $\Delta E^{0\,K}_{sub}(\omega_2) = 132.5$ kJ mol^{-1} and $\Delta H_{sub}(\omega_1) = 155.6$ kJ mol^{-1}, $\Delta H_{sub}(\omega_2) = 159.5$ kJ mol^{-1}. These values are in fair agreement with experiments: 142 ± 5 kJ mol^{-1}. This agreement with experiment at least proves that the structures we proposed for both allotropes are certainly *among the lowest ones in energy*. In ω_1-sulfur the consideration of a ten atom per elementary helix cell structure would have led to 114.7 kJ mol^{-1}.

In fact, a more detailed analysis has to be made. Since weak heating transforms $S_{\omega 2}$ into $S_{\omega 1}$, while $S_{\omega 2}$ is naturally produced in syntheses (at low temperatures), we may state that $S_{\omega 2}$ is the *kinetic product* and $S_{\omega 1}$ is the *thermodynamic product*. The ΔC_p in Fig. 10 is the difference between the C_p corresponding to the condensed phase and that of S_8 and the numerical value is obtained by integration. For the condensed phase, the curve $C_p = f(T)$ has been previously published[32] and an accurate theoretical determination has been used for S_8.[30] For the condensed phase, a peak around liquid nitrogen temperature is characteristic of a phase transition and then up to 298 K we probably have more and more $S_{\omega 1}$ instead of $S_{\omega 2}$. Therefore, the ΔC_p value given in Fig. 10 certainly is more appropriate for $S_{\omega 1}$ than for $S_{\omega 2}$. Above the transition phase, $S_{\omega 2}$ is a metastable compound. Only particular (and difficult) experimental conditions would allow the determination of $C_p = f(T)$ for this allotrope up to the ambient temperature. In conclusion, the $\Delta H_{sub}(\omega_2)$ value given above is slightly less accurate than the $\Delta H_{sub}(\omega_1)$ value. Of course, the relative stabilities found at 0 K were not concerned by these thermodynamic considerations.

Conclusions

The precise determination of the allotropes of ω-sulfur is difficult because of both the structural complexity of the systems and the necessity to represent the weak forces between helices of sulfur atoms. We bypassed the theoretical problem by adding a dispersion energy calculation to a tractable semi-empirical quantum mechanical method. For the first difficulty, we proceeded step-by-step, from 1D (two isolated infinite helices) to 2D (an infinite linear row of infinite helices) and finally to the real 3D structures, taking advantage of the preceding results to limit the (tremendous) number of possible conformations to fewer possibilities in the next step. We conclude that the ω_2-sulfur allotrope is more stable than ω_1-sulfur at 0 K. Adding the EHT estimate of the energy difference between three and ten atoms per cell helical chains, only reverse the relative stabilities in the case of 1D structures. Let us notice that this difference, very small, *has no influence at all* in the thermodynamic discussion.

Starting from the general structural schemes proposed from experiments, we have obtained new information both for theoretical and structural points of view. Having linked the number of atoms in the elementary cell and the assumed 'experimental' value of the interatomic S—S distance between neighbouring atoms to the c crystallographic index (ω_1 case) and to the a and b indices (ω_2 case), the remaining indices have been optimized to reach minima of total energy in the two cases. For the retained values of $S_{\omega 1}$ (see Table 4), a_{min} and b_{min} overestimate the experimental values ($a = 9.02$ Å; $b = 8.32$ Å) by only 5.3% and 8.1%, respectively. For $S_{\omega 2}$ (see Table 6), the retained c_{min} index, equal to four times the R_{min} value, underestimates by only 4.4% the experimental value ($c = 16.32$ Å). This is a fair agreement with experiment.

By considering the repulsive part only, it is not possible to reproduce in all cases the shifts along the helix axis as found after addition of the dispersion energy. But for a given shift, it leads to a correct estimate of the angles of rotation between helices. Of course, dispersion energy is of vital importance for determining the minimum in the interaction energy maps, leading to the crystalline parameters a and b. Taking into account C_6 terms only would have led to a very weak cohesion. The introduction of C_8 and three-body terms has proved to be of vital importance. Moreover, 1D and 2D model structures are not sufficient to simulate successfully the real structures of $S_{\omega 1}$ and $S_{\omega 2}$.

We may state that one of the stable conformations of $S_{\omega 2}$ is built from parallel planes of helices (axes of helices in one plane are perpendicular to those of helices in the next neighbouring plane) with three atoms per elementary cell in one helix. This number of atoms was also a characteristic of $S_{\omega 1}$, a more simple structure than $S_{\omega 2}$ since it is constituted of parallel helices. Another common point is the shift, along the helix axis, between neighbouring helices. In all cases the most stable structure is the one with $q = 1/2$, that is a shift equal to one-half the height of the second atom relative to the first. In Part I, Fig. 8, showing the interpenetration of two helices for $q = 1/2$, in the 1D example treated, was particularly illuminating. In addition, we have also to point out that only for $N_{ec} = 3$, did we find a 3D structure more stable than the corresponding 2D structure. For ten atoms per elementary helical cell, this was not the case.

Our results are consistent with recent experiments concerning the preparation of polymeric sulfur and the determination of enthalpies of sublimation from the study of the vapour in equilibrium with the solid.

Acknowledgements

We would like to thank the Centre National Universitaire Sud de Calcul (CNUSC, Montpellier, France) for computing facilities, and at the CTM (Marseille): Dr Francis Marinelli for helping us in CRYSTAL program runs, Dr Claire Bergman for the discussion concerning thermodynamic measurements and Mr Marcel Gilbert, in charge of the computing equipment.

References

1 F. Cataldo, *Angew. Makromol. Chem.*, 1997, **249**, 137.
2 (*a*) *Elemental Sulfur, Chemistry and Physics*, ed. B. Meyer, Interscience, New York, 1965; (*b*) B. Meyer, *Adv. Inorg. Chem. Radiochem.*, 1976, **18**, 287; (*c*) B. Meyer, *Chem. Rev.*, 1976, **76**, 367; (*d*) J. Donohue, *The Structures of the Elements*, Wiley, New York, 1974.
3 S. R. Das, *Indian J. Phys.*, 1938, **12**, 163.
4 O. Erametsa, *Suomen Kemistilehti*, 1963, **B36**, 213.
5 F. Tuinstra, *Physica*, 1967, **34**, 113.
6 L. Pauling, *Proc. Natl. Acad. Sci. USA*, 1949, **35**, 495.
7 Y. Olkhov and B. Jurkowski, *J. Appl. Polym. Sci.*, 1997, **65**, 499.
8 (*a*) F. Michaud, Thesis, Université de Montpellier II, 1989; (*b*) F. Michaud, J. Fourcade, E. Philippot, M. Maurin and M. Discours, *Proceedings of the International Symposium on Elemental Sulfur in Agriculture*, Syndicat Française du Soufre, Marseille, 1987, vol 2, p. 789.
9 (*a*) J. A. Prins, J. Schenk and L. H. J. Wachters, *Physica*, 1957, **23**, 746; (*b*) J. A. Prins and F. Tuinstra, *Physica*, 1963, **29**, 884.
10 F. Tuinstra, Thesis, *Structural aspects of the allotropy of sulfur and the other divalent elements*, V. Waltmann, Delft, 1967.
11 (*a*) M. D. Lind and S. Geller, *J. Chem. Phys.*, 1969, **51**, 348; (*b*) S. Geller and M. D. Lind, *Acta Crystallogr., Sect. B*, 1969, **25**, 2166.
12 M. Springborg and R. O. Jones, *Phys. Rev. Lett.*, 1986, **57**, 1145.
13 A. Karpfen, *Chem. Phys. Lett.*, 1987, **136**, 571.
14 C. X. Cui and M. Kertesz, *J. Am. Chem. Soc.*, 1989, **111**, 4216.
15 D. S. Warren and B. M. Gimarc, *J. Phys. Chem.*, 1993, **97**, 4031.
16 M. Ezzine, A. Pellegatti, C. Minot and R. J.-M. Pellenq, *J. Phys. Chem. A*, 1998, **102**, 452.
17 R. Hoffmann, *J. Chem. Phys.*, 1963, **39**, 1397.
18 M. J. S. Dewar, Y. Yamaguchi and S. H. Suck, *Chem. Phys.*, 1979, **43**, 145.

19 M. Ezzine, R. Chastel and C. Bergman, *J. Alloys Comp.*, 1995, **220**, 206.
20 (*a*) M.-H. Whangbo and R. Hoffmann, *J. Am. Chem. Soc.*, 1978, **100**, 6093; (*b*) C. Minot, M. A. van Hove and G. A. Somorjai, *Surf. Sci.*, 1983, **127**, 441.
21 C. Vidal-Madjar and C. Minot, *J. Phys. Chem.*, 1987, **91**, 4004.
22 R. J.-M. Pellenq, A. Pellegatti, D. Nicholson and C. Minot, *J. Phys. Chem.*, 1995, **99**, 10175.
23 (*a*) R. Hoffmann and P. Hofmann, *J. Am. Chem. Soc.*, 1976, **98**, 598; (*b*) J. H. Ammeter, H. B. Burgi, J. Thibeault and R. Hoffmann, *J. Am. Chem. Soc.*, 1978, **100**, 3686; (*c*) M.-H. Whangbo and R. Hoffmann, *J. Chem. Phys.*, 1978, **68**, 5498.
24 It is well-known that, the greater the size of the elementary cell, the lower is the number of $\boldsymbol{k}$ points necessary to obtain a good accuracy for the energy. Indeed, for large unit cells, the band dispersion is weak and the calculations can be performed at a single point of the Brillouin zone. The origin of the Brillouin zone, the Γ point, is usually chosen. Here, when $N_{ec} = 10$, we have made this choice, which is no longer valid for $N_{ec} = 3$ where more $\boldsymbol{k}$ points are needed.
25 (*a*) R. J.-M. Pellenq and D. Nicholson, *J. Phys. Chem.*, 1994, **98**, 13339; (*b*) R. J.-M. Pellenq, PhD Thesis, Imperial College, University of London, 1994; (*c*) D. Nicholson, A. Boutin and R. J.-M. Pellenq, *Mol. Simul.*, 1996, **17**, 217.
26 K. T. Tang, J. M. Norbeck and P. R. Certain, *J. Chem. Phys.*, 1976, **64**, 3063.
27 K. T. Tang and J. P. Toennies, *J. Chem. Phys.*, 1984, **80**, 3726.
28 R. J.-M. Pellenq and D. Nicholson, *J. Chem. Soc., Faraday Trans.*, 1983, **89**, 2499.
29 G. Moretti, *Surf. Interface Anal.*, 1990, **16**, 159.
30 M. Ezzine, Thesis, Université de Provence, Marseille, 1992.
31 We checked that, for $N_{ec} = 3$, it is necessary to take $n_k = 8$ (in the *a* and *b* directions) in order to obtain the same accuracy as previously. On the other hand, for $N_{ec} = 10$, we have 120 atoms in the elementary cell, and using only the Γ point we obtain five exact decimals in the interaction energy.
32 J. C. Van Miltenburg, J. Fourcade, M. Ezzine and C. Bergman, *J. Chem. Thermodyn.*, 1993, **25**, 1119.
33 (*a*) R. Dovesi, C. Pisani, C. Roetti, M. Causà and V. R. Saunders, *CRYSTAL 88*, *QCPE Program No. 577*, Bloomington, Indiana, 1989; (*b*) R. Dovesi, V. R. Saunders and C. Roetti, *CRYSTAL 92 User Documentation*, Torino and Daresbury, 1992; (*c*) C. Pisani, R. Dovesi and C. Roetti, in *Lecture Notes in Chemistry*, Springer-Verlag, Heidelberg, vol. 48, 1988.
34 The exponents of these d functions have been chosen equal to 0.59 (in S_8) and 0.65 (in $S_{3(\infty)}$), as in previous calculations of this type concerning sulfur.
35 The total energies from CRYSTAL 92 are $E(S_8) = -3180.0127$ a.u. and $E(S_{3(\infty)}) = -1192.4915$ a.u.

Received in Montpellier, France, 17th April 1998;
Paper 8/05084H